Retrieving the energy band of Cu thin films using quantum well states

2008 J. Phys.: Condens. Matter 20 035213

(http://iopscience.iop.org/0953-8984/20/3/035213)

J. Phys.: Condens. Matter **20** (2008) 035213 (6pp) doi:10.1088/0953-8984/20/03/035213

Retrieving the energy band of Cu thin films using quantum well states

J Wu[1], J Choi[1], O Krupin[2], E Rotenberg[2], Y Z Wu[1,3] and Z Q Qiu[1]

[1] Department of Physics, University of California Berkeley, Berkeley, CA 94720, USA
[2] Advanced Light Source, Lawrence Berkeley National Laboratory, Berkeley, CA 94720, USA
[3] Surface Physics Laboratory (National Key Laboratory), Fudan University, Shanghai 200433, People's Republic of China

Received 16 July 2007, in final form 27 November 2007
Published 17 December 2007
Online at stacks.iop.org/JPhysCM/20/035213

Abstract

Angle-resolved photoemission electron spectroscopy (ARPES) measurement was performed on epitaxially grown Cu/Co/Cu(001) films to observe the quantum well (QW) states due to the electron confinement inside the Cu film by the Cu/Co and Cu/vacuum interfaces. By studying the in-plane dispersion of the QW states, we find a nearly isotropic electronic structure in the neck region of the Fermi surface. Based on the quantization condition, we achieve a model-free method for obtaining the copper energy band $E(k_\perp, k_\parallel)$ and the energy contour near the Fermi energy. The result is in good agreement with theoretical calculations of the bulk copper energy band, showing that there is no significant difference in the energy bands between the bulk and thin film copper. This method can be generalized to measure energy bands of other metallic films using the QW states.

(Some figures in this article are in colour only in the electronic version)

1. Introduction

Electronic structure and electron energy bands of materials are key components in determining materials' properties. For nanostructures such as quantum dots, wire, and thin films, the reduced dimensionality and the presence of surfaces and interfaces could have a significant effect on the energy bands of a material and hence modify its properties [1]. The challenge in determining the energy bands of a nanostructure, such as a Cu ultrathin film, comes from the fact that the sample size is usually too small to generate enough signal in experiment [2]. This difficulty can be overcome with the development of some surface-sensitive measurement techniques such as angle-resolved photoemission electron spectroscopy (ARPES) whose typical detection depth is about a few atomic layers. In addition to the experimental difficulty, retrieving the energy bands from the experimental data also encounters the problem that data analysis is often somewhat model-dependent. The cause is that the electron momentum in the normal direction is not conserved in the ARPES process so that certain assumptions or models have to be applied to obtain the perpendicular component of electron momentum. This problem makes it difficult to obtain a reliable or model-free energy band in experiment. In this paper we present a method of obtaining the energy band of an ultrathin Cu film from the quantum well (QW) states as a solution to the above problem.

As is well known, the electron confinement in the normal direction of a nanometer thick metallic film leads to the formation of QW states to modulate the density of states (DOS) near the Fermi level [3], giving rise to a number of important phenomena such as the oscillatory magnetic interlayer coupling [4, 5], the magnetic anisotropy [6], and the stability of the so-called magic thickness [7], etc. Experimentally, ARPES provides the most direct observation of the QW states below the Fermi level. Since the photoemission intensity is roughly proportional to the DOS of the occupied electrons, the formation of QW states at discrete energy levels manifests itself as peaks in the photoemission energy spectrum. As required by the quantization condition, the positions of these QW peaks in the energy spectrum should evolve continuously with the film thickness. In particular, the photoemission intensity at a fixed energy should oscillate with the film thickness due to the presence of the QW states. Thus, counting the oscillation periodicity as a function of the film thickness enables the determination of the out-of-plane component of the electron momentum for that given electron energy. Since there is a simple relation between the in-plane component of the electron momentum and the

off-normal photoemission angle; the energy dispersion as a function of the in-plane component of the electron momentum can be measured by changing the off-normal photoemission angle. With the knowledge of all $(E, k_\perp, k_\parallel)$ sets, we can easily construct the energy band and the energy contour below the Fermi energy. The great advantage of this method is that the energy band determined in this way does not depend on any particular assumption or model of the metallic film in the sense that the key equation used in this method is the quantization condition from elementary quantum mechanics. In fact, obtaining the energy band from QW states has been practised in recent years. But because of the limited number of samples with different thicknesses, retrieving the energy band is usually achieved by data fitting with an energy-dependent phase in the electron quantization condition [8–11]. Model-free determination of the $k_\perp$ by counting the QW thickness oscillation periodicity is made only in a few cases for the normal emission ($k_\parallel = 0$) [12]. For the off-normal emission, retrieving the energy band has not been realized, to our best knowledge, by using a model-free method. The combination of the high spatial resolution (∼50 μm) of ARPES and the wedge-sample growth ability enables us to carry out a systematic study of the QW states as a function of the electron energy and the film thickness for both normal and off-normal photoemission. As shown in this paper, at each energy and off-normal angle, we are able to determine $k_\perp$ accurately with more than 100 film thicknesses from the QW state oscillations. This allows us to determine the Cu energy bands using a model-free method for both normal and off-normal directions.

2. Experiment

A Cu(001) single crystal was prepared by mechanical polishing down to a 0.25 μm diamond paste finish followed by electrochemical polishing [13]. Then the Cu substrate was cleaned *in situ* with cycles of Ar ion sputtering at 1.5 keV and annealing at 600–700 °C until sharp low energy electron diffraction spots were observed. The Co and Cu films were grown at room temperature by molecular-beam epitaxy. The growth rate was measured by a quartz crystal oscillator. The base pressure was about 1×10^{-10} Torr, and the pressure during the film growth was about 1×10^{-9} Torr. A 10-monolayer (ML) Co film was first grown uniformly onto the Cu(001) substrate to serve as the ferromagnetic substrate. Then a Cu wedge ranging from 0 to 25 ML with a slope of 5 ML mm^{-1} was grown on top of the Co for the QW states study. Both Co and Cu films are grown in the ordered layer-by-layer growth mode [14]. After the growth, the sample was transferred *in situ* to a measurement chamber to perform the photoemission experiment.

The ARPES measurement was carried out at beamline 7.0.1.2 of the advanced light source (ALS) of the Lawrence Berkeley National Laboratory. The small beam size (∼50 μm) gives a thickness resolution of ∼0.25 ML on our wedged sample. 83 eV photon energy was used to select the electronic states near the belly of the Cu Fermi surface. The photoemission electrons were collected by a Scienta SES-100 analyzer which simultaneously measures the energy and angular spectra. The angular window for the photoemission spectra is ∼40°. For the rest of the paper, the Fermi energy is defined as zero for convenience.

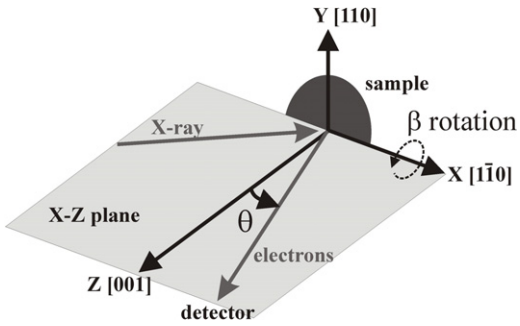

Figure 1. Schematic drawing of the ARPES measurement geometry. Z axis is the sample normal direction that is along the Cu [001] axis. X and Y axes are along Cu [1$\bar{1}$0] and [110] axes, respectively. θ and β represent the rotation angle around the Y and X axes, respectively.

3. Results and discussions

We first present the photoemission result in the energy and the off-normal angle plane at a fixed Cu thickness of 14 ML (figure 2). Figure 1 sketches the ARPES measurement setup with the Cu sample being aligned in such a way that θ and β denote the rotations around the Cu in-plane [110] and [1$\bar{1}$0] directions, respectively. Since the Cu [001] axis corresponds to the sample normal direction, a θ-scan (or β-scan) provides information about the energy band in the Cu(110) plane (or in the (1$\bar{1}$0) plane). Thanks to the Scienta SES-R4000 analyzer, which measures simultaneously the energy spectrum and the θ-scan from $-20°$ to $+20°$, a single measurement of the β-scan by mechanically rotating the sample allows the collection of the entire energy spectra in the θ–β plane. Figure 2(a) shows the photoemission energy spectrum at the normal emission ($\theta = \beta = 0°$). The first thing we noticed in figure 2(a) is that there are three peaks with energies -0.07, -0.71 and -1.33 eV below the Fermi energy. Recall that the photoemission intensity is proportional to the number of electrons in the occupied state, the appearance of the photoemission peaks in the energy spectrum corresponds to a favorite population of electrons at certain energy levels—a signature of the QW states in the Cu thin film.

Electrons in a Cu layer form QW states due to the confinement by both an imaging potential at the vacuum/Cu interface due to electron–hole attraction and the minority-spin band of the Co at the Cu/Co interface. The quantization is usually modeled as an electron in a potential well of width d_{Cu} with the quantization condition of:

$$2k_\perp d_{\mathrm{Cu}} + \phi_{\mathrm{C}} + \phi_{\mathrm{B}} = 2\pi n \qquad n = \text{integer} \qquad (1)$$

where $k_\perp$ is the out-of-plane component of the electron's momentum, d_{Cu} is the copper film thickness, ϕ_{B} and ϕ_{C} are phase gains of the electron wavefunction at the vacuum/Cu and Cu/Co interfaces, respectively. By taking the Cu thickness as

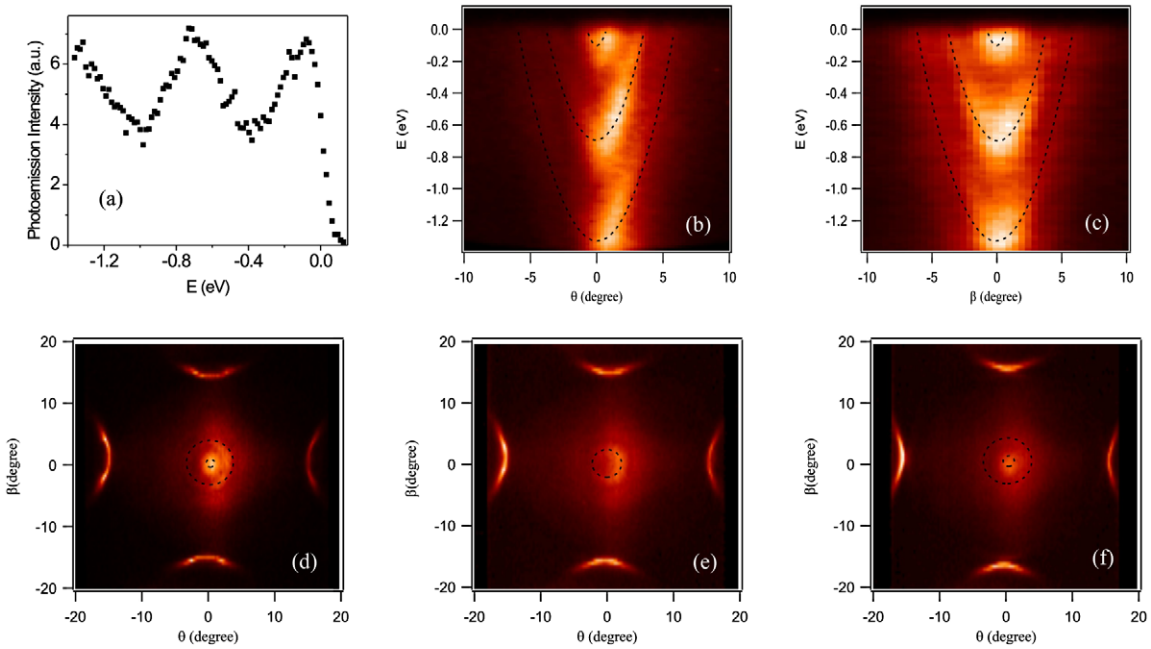

Figure 2. The photoemission intensity (a) as a function of the electron energy at the normal emission, (b) in the E–θ plane, (c) in the E–β plane, (d) in the θ–β plane at $E = -0.07$ eV, (e) in the θ–β plane at $E = -0.35$ eV, and (f) in the θ–β plane at $E = -0.71$ eV. The dashed lines are guides to the eye.

integer multiples (m) of the atomic spacing ($a = 1.8$ Å along [001]), equation (1) can be rewritten in terms of a new index ν:

$$2k_{\perp}^{e} d_{Cu} - \phi_C - \phi_B = 2\pi\nu \tag{2}$$

where $k_{\perp}^{e} = k_{BZ} - k_{\perp}$, $k_{BZ} = \pi/a$ (the Brillouin-zone (BZ) vector), and $\nu = m - n$ is the new index. Equations (1) and (2) are identical for $d_{Cu} = ma$ but $k_{\perp}^{e}$ now decreases with energy as observed in experiment [15]. The quantization condition selects discrete $k_{\perp}^{e}$ values for a given Cu thickness, which satisfies $k_{\perp}^{e} = (2\pi\nu + \phi)/2d_{Cu}$, where $\phi = \phi_C + \phi_B$. Then the momentum–energy correspondence (the energy dispersion relation will be discussed later in this paper) specifies the quantized energy levels as observed in figure 2(a). It can be further concluded that the QW peak positions in the energy spectrum should also depend on the accumulated phase ϕ and the Cu film thickness.

We then did angle-resolved photoemission measurements as a function of both θ and β at a fixed Cu thickness of 14 ML. Figures 2(b) and (c) display the photoemission intensity in the E–θ and E–β planes. Three pieces of information can be obtained from the above two figures. First, the QW peaks at normal emission also exist at off-normal angles though their intensities become weaker with increasing angle. Second, the QW states behave exactly the same in the E–θ and E–β planes, which is not surprising because the θ and β scans correspond to two equivalent in-plane crystal axes of [110] and [1$\bar{1}$0], respectively. Finally, the QW peaks evolve into a parabola shape (denoted with the dashed line in figures 2(b) and (c)) as a function of the off-normal angle. Note that the electron in-plane momentum ($k_{\parallel}$) is related to the off-normal angle with

$$k_{\parallel} = \frac{\sqrt{2m_e(h\nu - W - |E|)}}{\hbar} \cdot \sin\theta \qquad (\text{or } \sin\beta). \tag{3}$$

Here m_e is the electron mass, $h\nu = 83$ eV is the photon energy, and $W = 4.46$ eV is the Cu work function [16]. The energy E is negative according to our definition. For small angle, $\sin\theta$–θ thus the parabolic curves in figures 2(b) and (c) actually describe the QW dispersion with the in-plane electron momentum.

$$E_F - |E| = E_F + E = \frac{\hbar^2 k_{\perp}^2}{2m_{\perp}^*} + \frac{\hbar^2 k_{\parallel}^2}{2m_{\parallel}^*}. \tag{4}$$

Here $m_{\perp}^*$ and $m_{\parallel}^*$ are the electron out-of-plane and in-plane effective masses. For every discrete $k_{\perp}$ value from equation (1), the QW energy is thus a quadratic function, as observed in figures 2(b) and (c). However, it is very easy to mistake the quadratic dispersion as a result of the second term of equation (4) only. The reason is that $k_{\perp}$ also disperses with $k_{\parallel}$ so that both terms in equation (4) actually vary with $k_{\parallel}$. Therefore one has to be very careful in obtaining the electron in-plane effective mass from the quadratic fitting [17].

To further explore the dispersion of the QW states with the in-plane momentum, we plot the photoelectron intensity as a function of θ and β at fixed energy. The combination of θ and β covers all possible in-plane directions and gives a systematical study of the QW states versus the in-plane vector $\vec{k}_{\parallel}$. The θ–β plots at three different energies of -0.07 eV, -0.35 eV, and -0.71 eV are shown in figures 2(d)–(f). First, the four arcs near the edge of the figure are the result of the necks of the Cu Fermi surface projected in the θ–β plane. The neck is located at 15.0° of the off-normal angle which corresponds to $k_{\parallel} = 1.17\text{Å}^{-1}$ from equation (3), agreeing with the theoretical value [18]. In addition to the bulk features, we observe rings near the center of the BZ. These rings correspond to the QW states or the constant energy contours of the QW

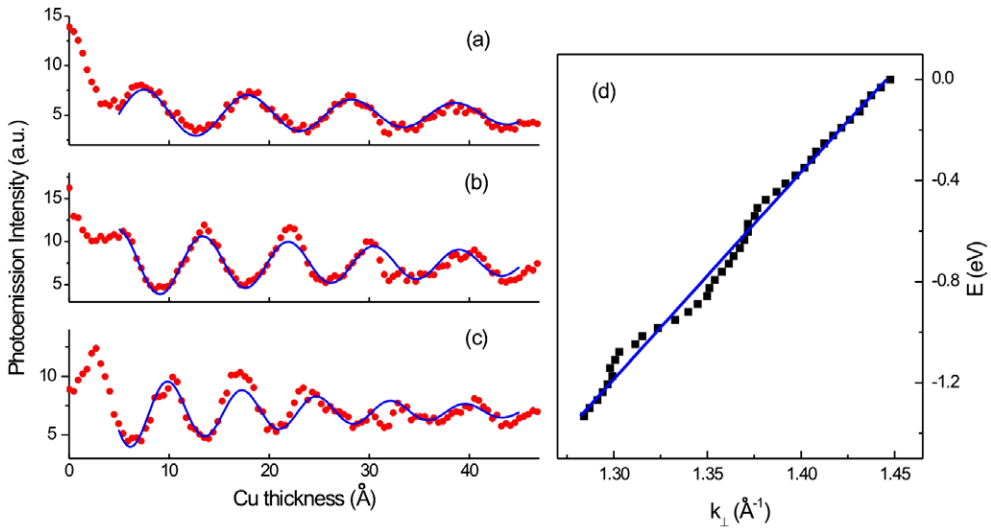

Figure 3. Photoemission intensity at normal emission as a function of Cu thickness at (a) 0.0 eV, (b) −0.5 eV, and (c) −1.0 eV. Solid lines are the fitting result from equation (5). (d) Energy dispersion obtained from experiment (dots) and fitting result (solid line) from equation (6).

states in the θ–β plane. This can be easily understood from equation (4) that quantized $k_\perp$ at a constant energy should lead to discrete values of $k_\parallel$. The interesting observation is that these QW rings have a constant radius, i.e. the $k_\parallel$ is independent of the in-plane direction in the θ–β plane. This result shows that the electron in-plane effective mass and the quantized out-of-plane momentum $k_\perp$ must be isotropic for any in-plane direction. The isotropic $m_\parallel^*$ indicates an isotropic Cu energy band with respect to the $k_\parallel$ near the Fermi surface at its [001] direction. The isotropic $k_\perp$ shows that the underlayer Co, which confines the Cu electron to quantize the $k_\perp$, also processes an isotropic energy band with respect to the near [001] direction. Another observation is that figures 2(d) and (f) have high photoemission intensity at the center of the θ–β plane and figure 2(e) has low photoemission intensity at the center. This result is consistent with the fact that figures 2(d) and (f) are taken at the QW peak energies of figures 2(a) and (e) is taken at the QW valley energy of figure 2(a).

Next, we present the measurement result of Cu/Co/Cu(001) along the Cu wedge. Figures 3(a)–(c) show the normal photoemission ($\theta = \beta = 0°$) intensity as a function of the Cu thickness at three representative energies. At the Fermi energy (figure 3(a)), the high intensity below ∼5 Å is due to the Co substrate which has a higher density of states at the Fermi level. Above the photoelectron escaping depth, the photoemission intensity develops regular oscillations as a function of the Cu thickness due to the QW states. This oscillation can be well described by a sinusoidal function with an exponentially decaying amplitude.

$$I = I_0 + A \cdot \exp(-d_{\mathrm{Cu}}/\mu) \cdot \cos[2(k_{\mathrm{BZ}} - k_\perp)d_{\mathrm{Cu}} - \phi]. \quad (5)$$

Here I is the photoemission intensity, A is the oscillation amplitude, μ is the characteristic decay length of the amplitude, and I_0 is the background intensity.

Using equation (5), we fit the experimental data to determine the $k_\perp$ value. It is worth pointing out that the phase ϕ is treated as a fitting parameter here although there are some model-dependent expressions $\phi(E)$ from the literature, e.g. the phase accumulation model (PAM) [19]. By freeing ϕ from any model-dependent value, the $k_\perp$ determined from the fitting will entirely depend on the oscillation periodicity rather than the model-dependent expression of $\phi(E)$, i.e. the $k_\perp$–E relation (or the energy band) obtained from our fitting does not require knowledge of the phase. The fitting result (solid lines in figures 3(a)–(c)) represents the experimental data very nicely in the thickness range studied, yielding $k_\perp = 1.45$ Å^{-1}, 1.38 Å^{-1}, and 1.32 Å^{-1} at $E = 0.0$ eV, −0.5 eV, and −1.0 eV, respectively. The $k_\perp = 1.45$ Å^{-1} at $E = 0.0$ eV agrees nicely with the literature value of the Cu Fermi wavevector [20]. Repeating this fitting procedure at other energies, we obtained the Cu energy band along the [001] direction (dots in figure 3(d)). As is well known, the Cu sp electrons near the Fermi energy can be well described by the nearly-free-electron model.

$$E(k) = \frac{\varepsilon_k + \varepsilon_{k-2k_{\mathrm{BZ}}}}{2} - \sqrt{\left(\frac{\varepsilon_k - \varepsilon_{k-2k_{\mathrm{BZ}}}}{2}\right)^2 + U^2}$$
$$\text{with } \varepsilon_k = \frac{\hbar^2 k^2}{2m^*}. \quad (6)$$

Here $2U$ is the energy gap at the BZ boundary and m^* is the effective mass of the electron. To test our methodology of obtaining the energy band from the QW states, we fitted the E–k relation from our experiment by the nearly-free-electron model using the measured Fermi wavevector k_{F} and two free fitting parameters of m^* and U. The fitting result (solid line in figure 3(d)) agrees very well with the experimental data, and yields the values of $m^* = 1.14 m_{\mathrm{e}}$ and $U = 3.4$ eV. In parallel, the phase ϕ as a function of the energy E is obtained from our data fitting as well and it is in modest agreement with the prediction of PAM. Since our result of the phase ϕ is the same as figure 5 of [21] where a detailed discussion of the phase ϕ can be found, we do not need to repeat the discussion here.

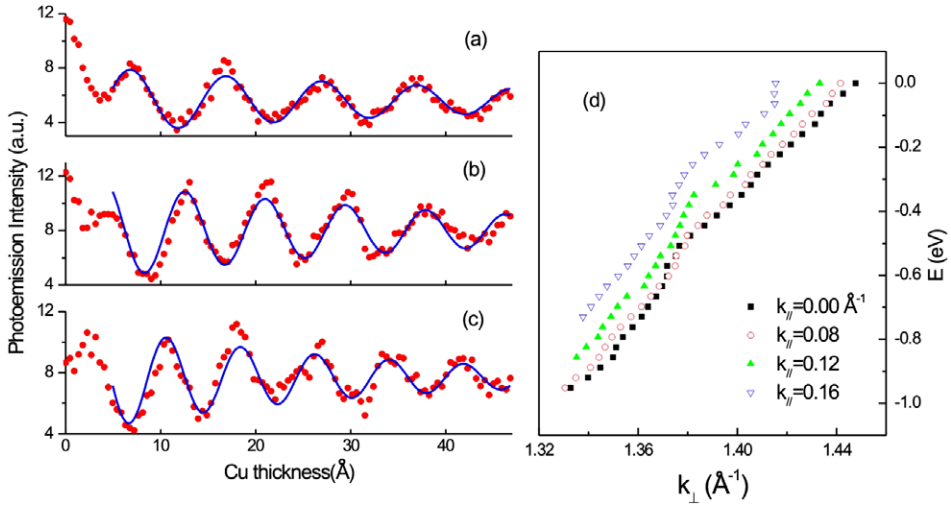

Figure 4. Photoemission intensity at $k_{\parallel} = 0.16$ Å^{-1} as a function of Cu thickness at (a) 0.0 eV, (b) −0.5 eV, and (c) −1.0 eV. Solid lines are the fitting result from equation (5). (d) Energy dispersion obtained from experiment at several $k_{\parallel}$.

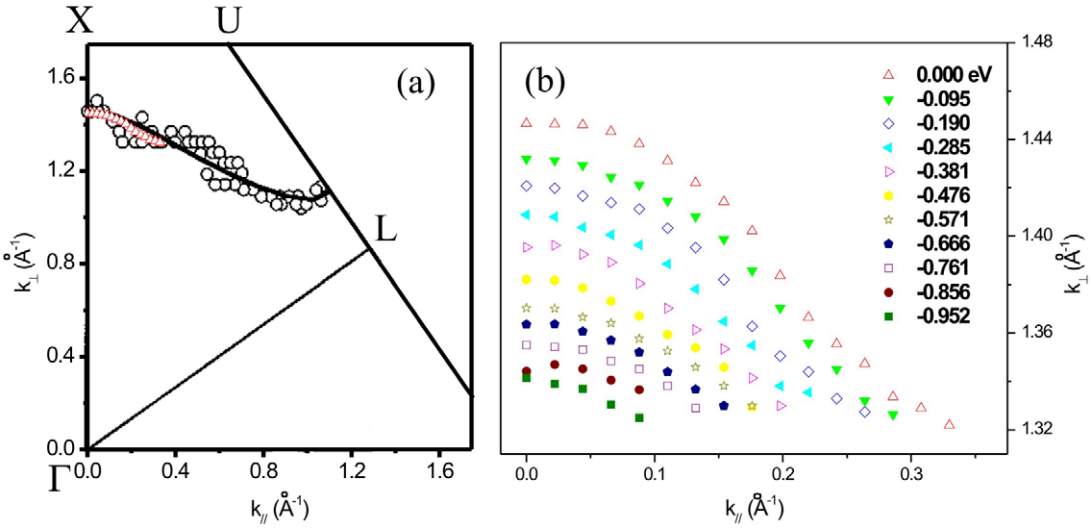

Figure 5. (a) The Fermi energy contour in the Cu(110) plane. Triangles are our experimental data. Circles and solid lines are from experiment and calculation of [13]. (b) The energy contours constructed from our experimental data in the Cu (110) plane.

After verifying the validity at normal emission, we applied this method to off-normal photoemission. Because of the isotropic electronic structure, as shown in figures 2(d)–(f), we only analyzed the off-normal photoemission data for the $\beta = 0°$ case. As an example, figure 4 presents the result for the case of $\theta = 2°$ ($k_{\parallel} = 0.16$ Å^{-1}). The raw data and the best fitting at electron energies of 0.0 eV, −0.5 eV, −1.0 eV were plotted in figures 4(a)–(c), respectively, with the oscillation periodicity determining the corresponding $k_{\perp}$. Figure 4(d) shows the $E - k_{\perp}$ relation obtained in this way at several representative $k_{\parallel}$. This method allows us to determine the energy band $E(k_{\parallel}, k_{\perp})$ at every $k_{\parallel}$ and $k_{\perp}$, thus offering a powerful tool for the study of the energy band of metallic thin films.

An alternative way of presenting the result is to construct the energy contours near the Fermi energy. At each fixed energy, we determine the $k_{\perp}$ from the oscillation periodicity of the Cu thickness at different off-normal angles. In this way, we can obtain the $(k_{\parallel}, k_{\perp})$ pairs for that given energy, or the energy contour in the BZ. By marking $(k_{\parallel}, k_{\perp})$ pairs of the Fermi energy, we are able to construct the Fermi energy contour (figure 5(a)). The solid line and circles in figure 5(a) are from a theoretical calculation and a previous experiment for bulk copper in the [110] plane [22]. The agreement between our experiment (represented by triangles) and the theory shows that there is no significant difference between the band structure of a copper thin film and bulk copper. Repeating this procedure at other energies, we construct the energy contour in the energy range of 0 to −1 eV for Cu thin film (figure 5(b)).

4. Summary

We performed MBE growth and *in situ* ARPES measurement on Cu/Co/Cu(001). From the Cu QW states and elementary

quantum mechanics, we develop a model-free analysis method to obtain the Cu energy bands and the energy contours. This method can be easily generalized to give a direct determination of the energy bands and energy contours for other metallic thin films using QW states.

Acknowledgments

This work was funded in part by the National Science Foundation under Contract No. DMR-0405259 and the US Department of Energy under Contract No. DE-AC03-76SF00098, and ICQS of the Chinese Academy of Science.

References

[1] Kittel C 2005 *Introduction to Solid State Physics* (New York: Wiley) chapter 17, 18
[2] Freeman A J 1969 *J. Appl. Phys.* **40** 1386
[3] Miller T, Samsavar A, Franklin G E and Chiang T C 1988 *Phys. Rev. Lett.* **61** 1404
[4] Ortega J E and Himpsel F J 1992 *Phys. Rev. Lett.* **69** 844
[5] Kawakami R K, Rotenberg E, Escorcia-Aparicio E J, Choi H J, Wolfe J H, Smith N V and Qiu Z Q 1999 *Phys. Rev. Lett.* **82** 4098
[6] Weber W, Bischof A, Allenspach R, Wursch Ch, Back C H and Pescia D 1996 *Phys. Rev. Lett.* **76** 3424
[7] Luh D A, Miller T, Paggel J J, Chou M Y and Chiang T C 2001 *Science* **292** 1131
[8] Paggel J J *et al* 2000 *Appl. Surf. Sci.* **162** 78
[9] Mugarza A *et al* 2004 *Phys. Rev.* B **69** 115422
[10] Schiller F *et al* 2004 *Phys. Rev.* B **70** 125106
[11] Zhang Y F *et al* 2005 *Phys. Rev. Lett.* **95** 096802
[12] Aballe L *et al* 2002 *Surf. Sci.* **518** 141
[13] Kawakami R K, Bowen M O, Choi H J, Escorcia-Aparicio E J and Qiu Z Q 1998 *Phys. Rev.* B **58** 5924
[14] Heinrich B *et al* 1991 *Phys. Rev.* B **44** 9348
[15] Kawakami R K, Rotenberg E, Escorcia-Aparicio E J, Choi H J, Cummins T R, Tobin J G, Smith N V and Qiu Z Q 1998 *Phys. Rev. Lett.* **80** 1754
[16] Anderson P A 1949 *Phys. Rev.* **76** 388
[17] Wu Y Z, Won C Y, Rotenberg E, Zhao H W, Toyoma F, Smith N V and Qiu Z Q 2002 *Phys. Rev.* B **66** 245418
[18] Burdick G A 1963 *Phys. Rev.* **129** 138
[19] Smith N V, Brookes N B, Chang Y and Johnson P D 1994 *Phys. Rev.* B **49** 332
[20] Coleridge P T and Templeton I M 1982 *Phys. Rev.* B **25** 7818
[21] An J M, Raczkowski D, Wu Y Z, Won C Y, Wang L W, Canning A, Van Hove M A, Rotenberg E and Qiu Z Q 2003 *Phys. Rev.* B **68** 045419
[22] Con Foo J A *et al* 1996 *Phys. Rev.* B **53** 9649